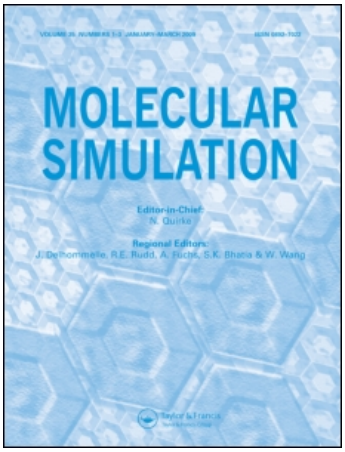

Molecular Simulation
Publication details, including instructions for authors and subscription information:
http://www.informaworld.com/smpp/title~content=t713644482

Molecular simulation of self-assembly of hydrophilic functionalized aromatics in aqueous solutions

S. Mohanty[a]
[a] Corporate Research Materials Lab, 3M Company, St Paul, MN, USA

To cite this Article Mohanty, S.(2006) 'Molecular simulation of self-assembly of hydrophilic functionalized aromatics in aqueous solutions', Molecular Simulation, 32: 8, 633 — 642
To link to this Article: DOI: 10.1080/08927020600887773
URL: http://dx.doi.org/10.1080/08927020600887773

Molecular Simulation, Vol. 32, No. 8, 15 July 2006, 633–642

Taylor & Francis
Taylor & Francis Group

Molecular simulation of self-assembly of hydrophilic functionalized aromatics in aqueous solutions

S. MOHANTY*

Corporate Research Materials Lab, 3M Company, St Paul, MN 55144-1000, USA

(Received April 2006; in final form June 2006)

This study identifies mechanisms of self-assembly of hydrophilic functionalized aromatic molecules—a distinct class of lyotropic materials. Results from molecular dynamics studies used to understand the moieties of the lyotropic molecule that affect the structure are consistent with experimental observations of these self-assembled structures. Coulombic forces, dominated by $\pi-\pi$ interactions drives the self-assembly of this class of materials. Intra-molecular configurations of the aromatic rings—the extent of torsion or bending between the rings—as well as the structure of functional groups connected to the rings affect the self-assembled structures. In addition, the chemistry of the functional groups also affects how the molecules are oriented as they self assemble. Molecular modeling provides insight into design of these molecules.

Keywords: Enthalpic-driven; $\pi-\pi$ Interactions; Multiscale order; Lyotropic

1. Introduction

Amphiphiles made up of hydrophilic and hydrophobic moiety form a family of self-assembling molecules. They are driven to self-assemble primarily by entropic changes in what is known as the "hydrophobic effect" [1]. The high cohesive energy of water causes the tails of the amphiphiles to cluster away from water (even though the interaction between the hydrocarbon tails and water is favorable) thereby minimizing disruption of interactions between water molecules. The head group interacts favorably with water and is at the interface of the cluster with water. Amphiphiles form lyotropic mesophases with the self-assembled structures being a function of concentration and temperature.

Another class of lyotropic materials is formed by hydrophilic functionalized aromatics (HFAs) [2]. These are mainly aromatic groups with functional groups attached to the periphery that can hydrogen bond or are polar. The aromatic groups stack owing to strong $\pi-\pi$ interactions. Thus, enthalpic contributions [3] are significant in ordering of these molecules. Aggregation is driven by what is termed as the "nonclassical hydrophobic effect".

These chemicals—many of them dyes and drugs—are critical in photosynthesis or in materials for manipulation of light only owing to their ability to self-assemble. Some of these HFAs stack into columns [2,4]. J-stacks have been observed in the self-assembly of a number of HFAs, first in aqueous solutions of pseudoisocyanine chloride (1,1′-diethyl-2,2′-cyanine chloride), also known as PIC. Others form helical structures [4,5]. Often, however, it is difficult to predict the behavior of these molecules as they self-assemble; small changes in functional groups can significantly change the self-assembling structure or even the ability to self-assemble. In addition, it has been difficult to predict the materials properties of these structures.

This study uses molecular dynamics methods to predict the self-assembled structures of some HFA molecules that have been studied quite extensively in the literature. The goal is to examine the ability of these methods to predict the self-assembled structures as well as to understand the mechanisms and thermodynamics of self-assembly. The structures of the molecules studied are shown in figure 1. The first three are a series of dyes of the 5,5′,6,6′-tetrachlorobenzimidacarbocyanine chromophore having 1,1′-dioctyl substituents combined with 3,3′-bis(4-carboxybutyl) or 3,3′-bis(3-carboxypropyl) substituents. The first is a 1,1′-diethyl-3,3′-bis (3-sulfobutyl) derivative abbreviated as TDBC. The second is a 1,1′-dioctyl-3,3′-bis(3-carboxypropyl)

*Email: smohanty@mmm.com

Molecular Simulation
ISSN 0892-7022 print/ISSN 1029-0435 online © 2006 Taylor & Francis
http://www.tandf.co.uk/journals
DOI: 10.1080/08927020600887773

substituted chromophore, as C8O3. The third is a 1′,1′-dioctyl-3,3′-bis(4-carboxybutyl) derivative which is abbreviated, as C8O4. The fourth is not a carbocyanine dye but rather an anti-asthmatic drug—disodium chromoglycate (DCNA)[6].

2. Simulation methods

This investigation was performed by using molecular dynamics algorithms within CERIUS2 with a dreiding force field that was optimized for water. Ten HFA molecules of a given kind (structure in figure 1) were randomly added to a unit cell of water (approximately 1000 molecules). This represents a concentration of over 10% by weight—a regime where these solutions begin to show lyotropic behavior. Significantly larger simulation systems become unviable vis-à-vis simulation time. Periodic boundary conditions were used during the simulation. Some of the snapshots are visualized such that the unit cells are placed periodically—this allows for visually identifying the continuity of stacks as they pass across unit cell boundaries. However, this also creates artificial appearance of order and we must be careful in our analysis. In addition, the boundaries of the unit cell also break up self-assemblies of longer length scales.

Following approximately 3000 steps of minimization, the system was allowed to equilibrate over 100,000 steps (equivalent to about 200 ps). The results presented are snapshots or averages after that period. Charge equilibration was performed on the system every 20,000 steps. Using two processors, the time for computation varied between 100 and 300 h depending on the number of molecules in the system; simulation of larger or more complex systems is unfeasible. The system does not reach equilibrium in that time-period; this is deduced from the continued decrease in energy with longer simulation time as well as significant differences in the details of the structures seen in these simulations when compared with experimental analysis. However, it becomes unfeasible to carry the simulation until global minimum—corresponding to a stable equilibrium structure—is attained. While the regularity of order that might be imagined at the equilibrium structure of a liquid crystal is not obtained, the trajectories for spontaneous self-assembly do provide significant understanding of the evolving lyotropic system. That is, these evolving simulations already show the nature of self-assembly that these molecules will attain

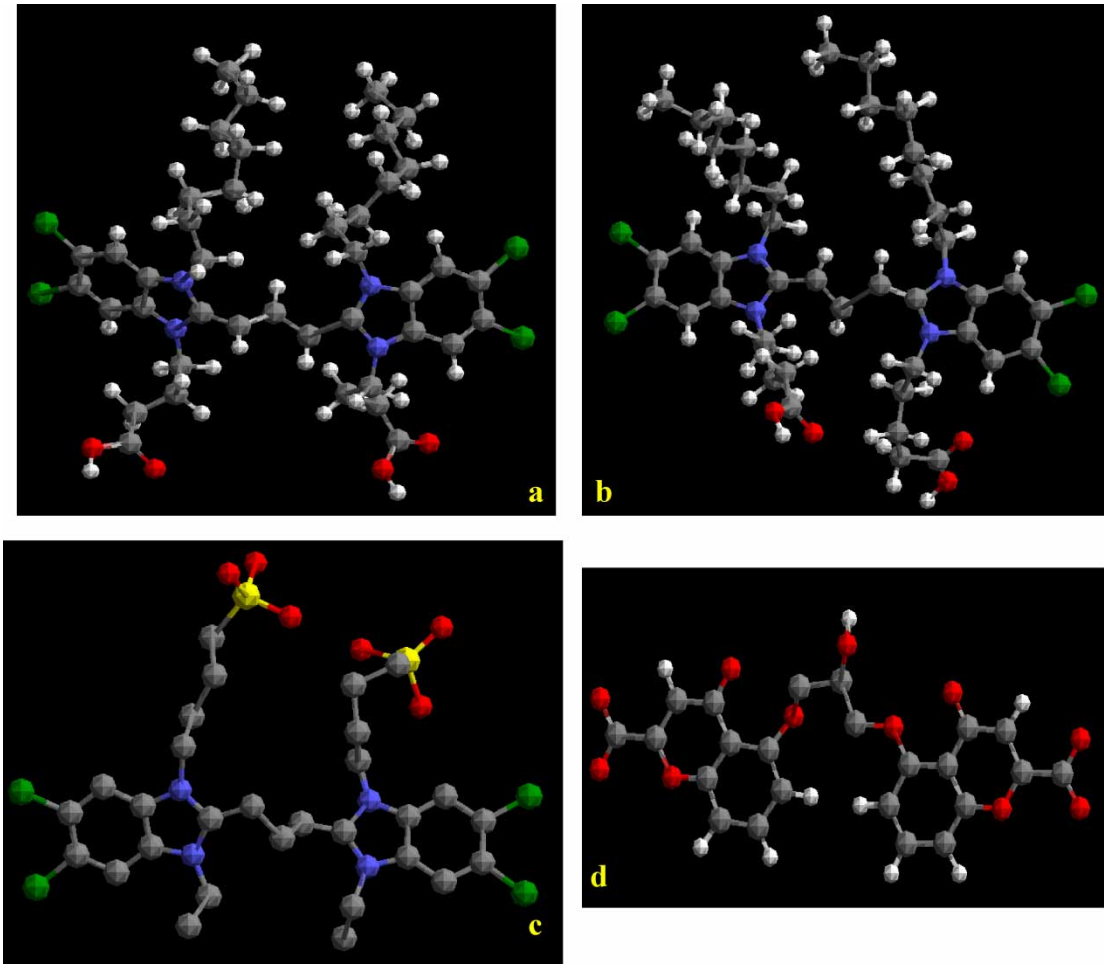

Figure 1. Molecular structures of: (a) C8O3; (b) C8O4; (c) TDBC; and (d) DCNA. The counter-ions—Br^- for the first two structures and Na^+ for the last two are not shown in the figure.

and the mechanisms that drive these self-assemblies, both of which provide valuable understanding.

3. Carbocyanine dyes

The carbocyanine dyes combine a highly delocalized π-electron system, which drives self-assembly owing to enthalpic considerations, with alkyl chains. Hence a strong effect on aggregation behavior and the resulting structure is to be expected. Experiments have observed that the solubility of these compounds in water is drastically reduced as are the threshold concentrations at which they form J-aggregates, when compared with PIC [4]. Despite similarity in structures, aqueous solutions of these molecules behave rather differently. Berlepsch *et al.* [4] observed that different starting stock solutions (of the same concentration) of TDBC and C8O4 gave identical absorption spectra (within experimental tolerances).

On the other hand, C8O3 displayed slightly different spectra even for freshly prepared solutions suggesting that the kinetics of self-assembly played a significant role in the self-assembled structure formed. Stock solutions of the three carbocyanine dyes showed optical anisotropy. C8O3 and C8O4 solutions showed a Schlieren-like texture on a millimeter scale within a day of preparation while TDBC showed birefringence only on stirring. An exact threshold for aggregation could not be measured but aggregation was visible at dye concentrations of about 10^{-5} M.

The visible absorption spectrum of TDBC in water shows a red-shift with respect to the monomer absorption band [7]. The absorption spectrum of C8O3, on the other hand, shows what is known as Davydov-split subbands. The J-aggregates of C8O3 show optical activity, indicating the formation of chiral aggregates [8,9,10]. The J-aggregates of C8O4 manifest spectral properties similar to TDBC. This is reflected in the circular dichroism of aqueous solution of these molecules [4]. Cryo-TEM show that TDBC aggregates into monolayer sheets, C8O3 forms "ropes" of helical stacks while C8O4 forms rod-like structures made up of striated bilayers.

4. Results: carbocyanine dyes

Simulations of aqueous solutions of the carbocyanine dyes listed above show clear evidence of spontaneous self-assembly. Randomly placed dye molecules begin to show correlated behavior over a short time scale of 200 ps. Snapshots of aqueous solutions of C8O3 are presented in figure 2. Tessellation of a few unit cells allows for the visualization of the self-assembly across unit-cell boundaries. Figure 2 shows that these molecules self-assemble into a twisting strand. A few of the molecules are magnified and show that they are ordered so as to facilitate interactions between the 6- and 5-membered rings between neighboring molecules. Each molecule is twisted at about 90° along the two-double bonds that link the conjugated rings. This allows for the formation of a chiral tube or strand. It is important to reiterate that this is not a snapshot of the equilibrium structure; rather it is a snapshot during the process of self-assembly. Experimental evidence agrees with chiral nature of these 1-D aggregates [4].

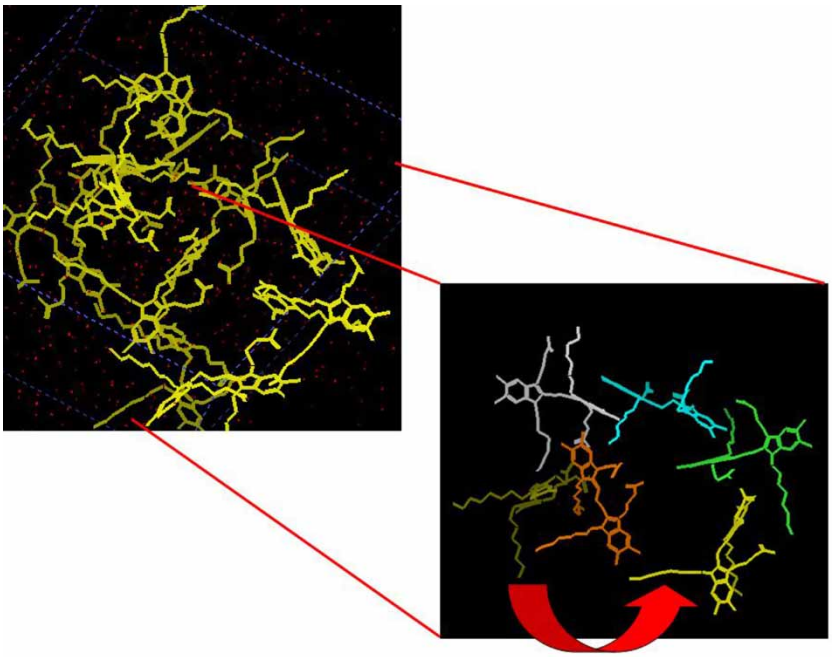

Figure 2. Snapshots of C8O3 molecules in water that are in the process of self-assembling. They show the chiral nature of the assembly. In the magnification, the molecules change their orientation in the same direction (the direction of the arrow) as one goes into the plane. In addition, the column itself twists (the dashed arrow)—the resulting phase looks like twisted ribbons.

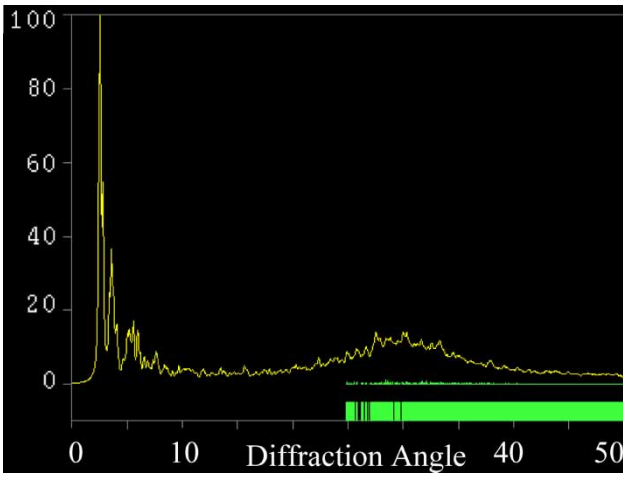

Figure 3. Simulated X-Ray diffraction pattern of self-assembled structure of C8O3 in water.

An X-ray diffraction pattern of the simulated structures is shown in figure 3. A broad peak at 29° corresponds to dimension of 0.3 nm. This is the distance between the aromatic rings in the self-assembly and points to the propensity for $\pi-\pi$ interactions. The higher intensity peaks at very small diffraction angles ($<5°$) represent the unit cell parameters. The slightly smaller peaks at about 6° represent a dimension of 1.5 nm, corresponding to the width of the strand. Experimental evidence based on light scattering and adsorption spectra of the dye [4] suggest a rod like self-assembly of this system with a mean width between 9 and 20 nm. Given the dimensions of the HFA molecule, this is possible only through an assembly of the helical wires similar to the results of these simulations. Experimental evidence also points to such an assembly of helical wires [4]. Given the limitations in computation speed and power, this simulation cell included only 10 HFA molecules. With such a small system, it is not possible to visualize the hierarchies in self-assembly suggested by optical techniques.

Figure 4 presents snapshots of an aqueous solution of C8O4 after 200 ps. The orthogonal view shows a structure that is undulating. Unlike experimental data that suggest that C8O3 and C8O4 behave differently [4], these simulations show similar helical structures. The diameter of the helix for C8O4 is slightly bigger. The bilayer structures that have been speculated to exist are not visible in these simulations [4]. It is possible that the simulations have not run long enough. However, given that the molecules show an internal twist at the conjugated double bonds linking the aromatic rings, the COO^- groups of each molecule are themselves pointed in different directions. Thus, if a bilayer (where COO^- groups of the two layers of the hydrocarbon groups of the two layers interact) exists, it must be in a complex form. The X-Ray diffraction pattern is similar to C8O3 with a broad peak at about 30° corresponding to about 0.3 nm—as with C8O3. Peaks showing the periodicity of the unit cell are also registered.

Figure 5 presents snapshots of TDBC in water. One orthogonal view shows a sheet like arrangement of the molecules; the other is a side view showing the thickness of the sheet as well as the spacing between them. A third view is a close-up of the self-assembled molecules highlighting the p–p interactions between the aromatic rings and the intra-molecular twist at the conjugated double bonds connecting the aromatic conjugates.

Measurements of the simulated self-assembly show each sheet to be about 2 nm thick which is compares rather well with estimates from SANS [4] at about 1.7 nm. The molecules are largely arranged in one plane. There is some effect from the size of the unit cell; bunching up of molecules along the unit cell boundaries is observed. The X-ray pattern of the structure again shows a broad peak at about 29°, which corresponds to the distance between aromatic rings (at about 0.3 nm). It also shows some sharp peaks at $<5°$ corresponding to the lattice parameters of the periodic cell. Another cluster of peaks is visible

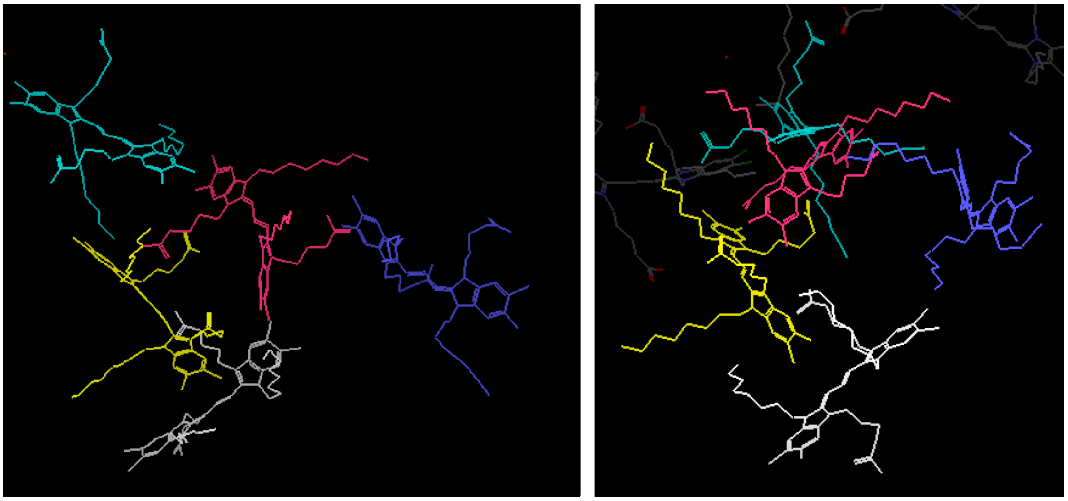

Figure 4. Snapshots of C8O4 molecules in water that are in the process of self-assembling. The left figure shows a single strand. The right figure shows a side view of that strand.

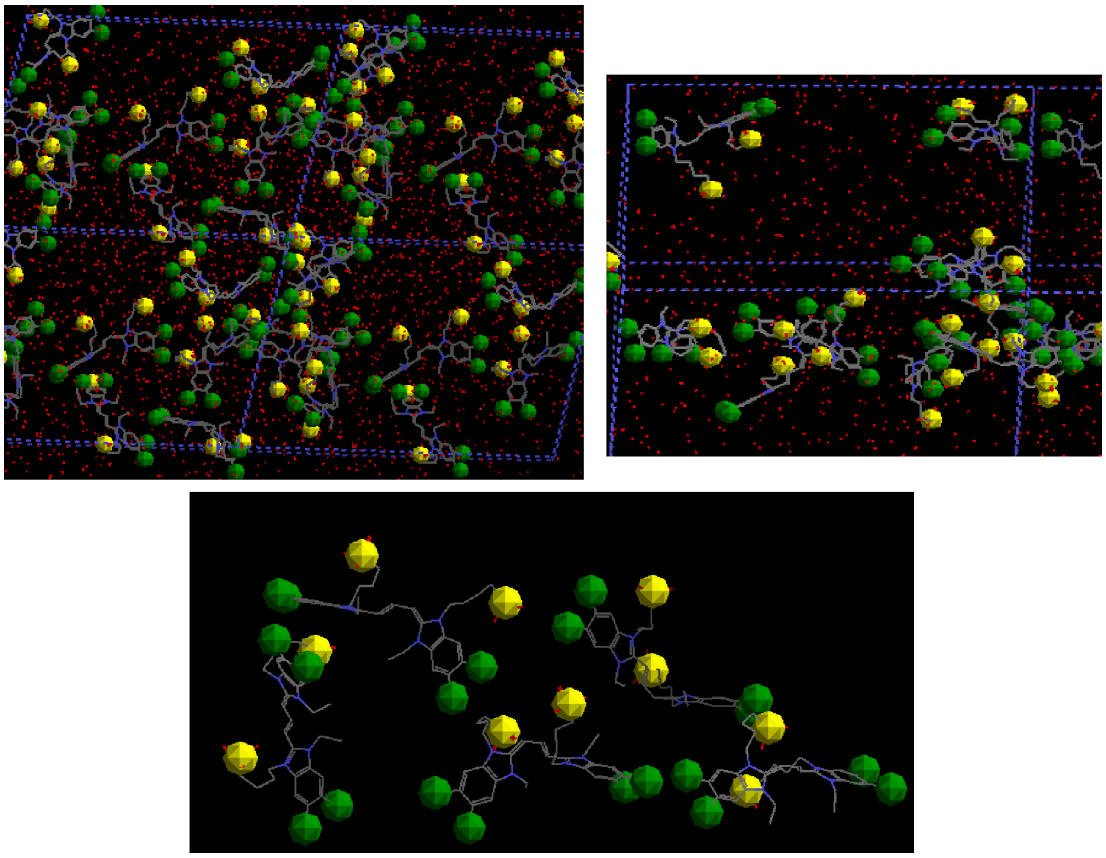

Figure 5. Orthogonal views of TDBC molecules in water in the process of self-assembling. They show the presence of sheets. The top left figure shows the top view of the sheet; the top right shows the side view with the thickness of each layer clearly visible. The bottom figure shows a snapshot of configuration of chromonics that form a flat layer.

between 5° and 6°, which is equivalent to a length of 1.5–1.7 nm. This dimension is the thickness of the sheet and is slightly different from the measured value (of 1.95 nm).

In figure 6, radial distribution functions of sulfur show that there are two other sulfur atoms in the neighborhood of any sulfur atom—one is the other sulfur atom connected to the molecule and the other is from a neighboring TDBC molecule. The radial distribution function of chlorine around sulfur is insightful. The distance between the nearest chlorine atoms and a sulfur atom in the same molecule is 0.8 nm. The other chlorine atoms are at about 1.5 nm from the sulfur atom. Yet, the radial distribution function shows a peak at about 0.4 nm and another at about 0.8 nm. Clearly, the chlorine atoms at 0.4 nm are from a neighboring TDBC molecule. The radial distribution functions thus provide further evidence of ordered aggregation.

The X-Ray spectra of all three self-assemblies are quite similar as shown in figure 7. Besides the peaks associated with the unit cell, each of these spectra shows a broad peak

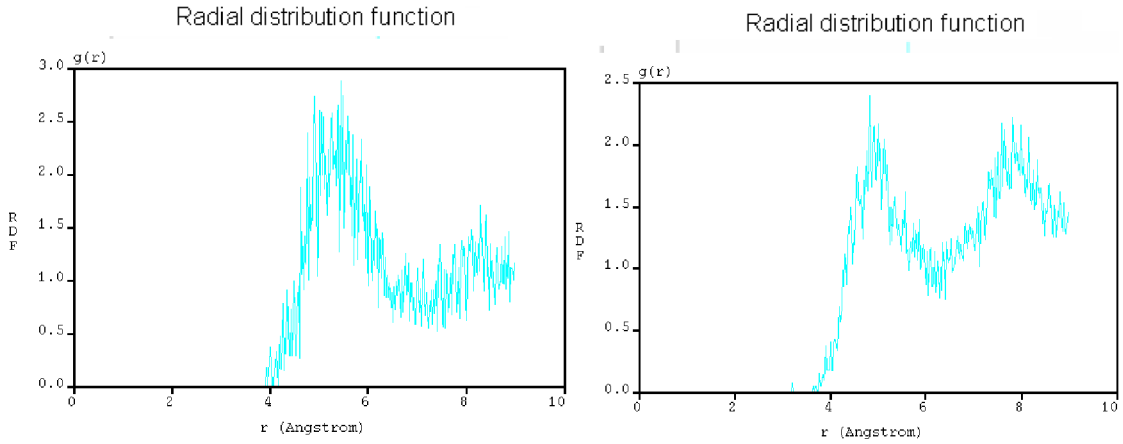

Figure 6. Radial distribution function of TDBC.

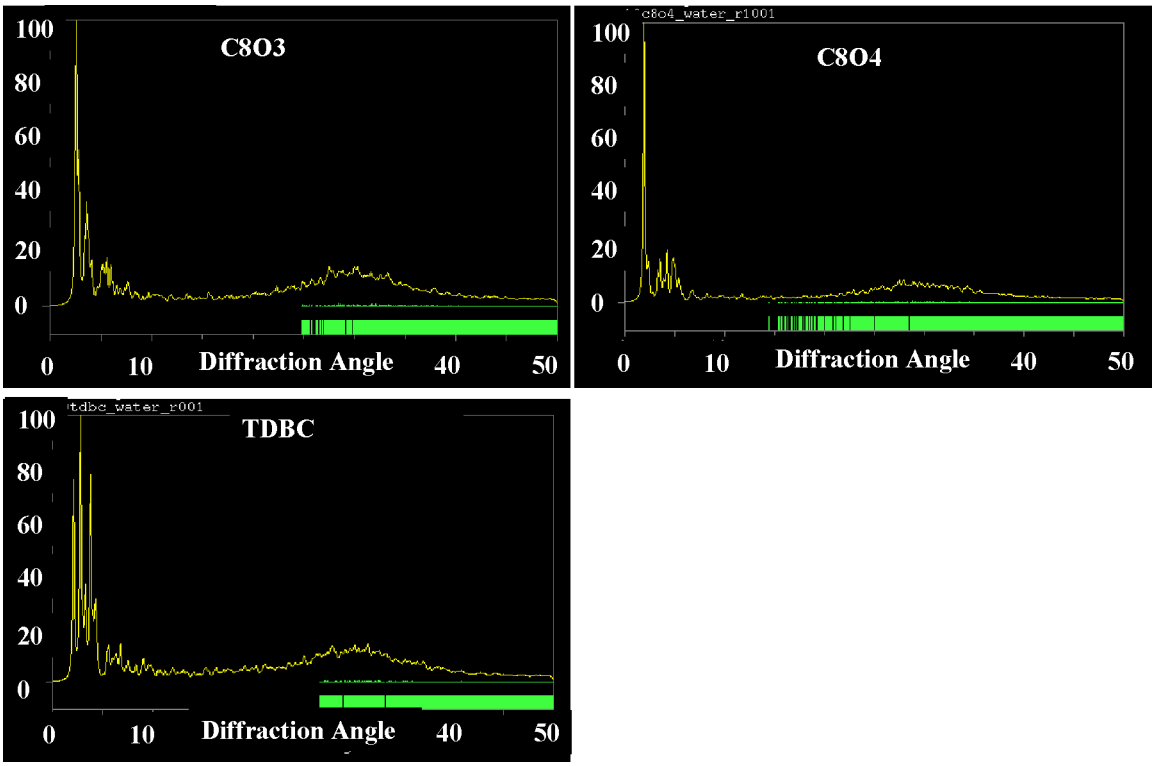

Figure 7. Comparison of X-Ray spectra of simulated self-assemblies of C8O3, C8O4 and TDBC.

at about 29° that is associated with the spacing between the aromatic rings as well as another peak that is associated with the thickness of a strand of these self-assembled molecules at about 1.7 nm. These features are common across the three self-assemblies even though the self-assemblies themselves are quite different.

While experiments suggest that the difference of one carbon in the side chains between C8O3 and C8O4 change the self-assembly structure significantly, that difference is not resolved in these simulations—perhaps pointing to the limitation of these relatively short simulations.

However, the difference between C8O3, C8O4 and TDBC is resolved by these simulations. Even though TDBC molecules also have a similar intra-molecular twist, the absence of a long side chain allows them to stay in planar self assemblies.

The importance of the molecular structure and its influence on self assembly is further highlighted by slightly changing the molecular structure. When the conjugated double bonds are removed—i.e. the aromatic conjugates are linked by a series of single bonds—none of the molecules self-assemble over similar periods of simulation time. At best, some dimers are seen where two neighboring molecules interact through their aromatic rings. This is true for TBDC, C8O3 and C8O4. The conjugated double bonds, while allowing for a twist in the planes of the two aromatic conjugates does not allow them to freely rotate with respect to each other. This constraint seems significant to self-assembly. When the double bonds are removed, self-assembly becomes unfeasible.

5. Results: sodium dichromoglycate

Figures 8 and 9 present snapshots of DCNA in water. X-Ray diffraction studies have shown that the nematic phase consists of cylinders that are approximately 2 nm in diameter and 20 nm in length [11]. Numerous configurations of DCNA have been suggested to explain their lyotropic behavior, including Lydon's claim that these molecules self-assemble into a cylinder with a cross-section that is a hollow square with the sodium ions forming salt bridges within the walls [12]. In fact, figure 8 shows two different views where the molecules are in the process of attaining their equilibrium structure. These structures suggest significantly different self-assembly behavior from the predictions of Kobayashi *et al.* [13]. In both these figures, one can see signs of the DCNA molecules twisting to form two different helical threads. It suggests that numerous helical threads co-twine; our small molecule simulation can only show two of them.

The sodium counter-ions lie outside, rather than within, the helical cylinder. The helix becomes more apparent when one looks at the placement and the changing orientations of the DCNA molecules labeled differently. The view along the length of the assembly shows two threads of four molecules each lying next to each other. Each molecule twists in a fashion that allows interactions between the aromatic rings of the neighboring molecule. Two threads that helically entwine are distinguished—one of them is labeled. The end on view also shows the intertwining of these threads. One can see the formation of

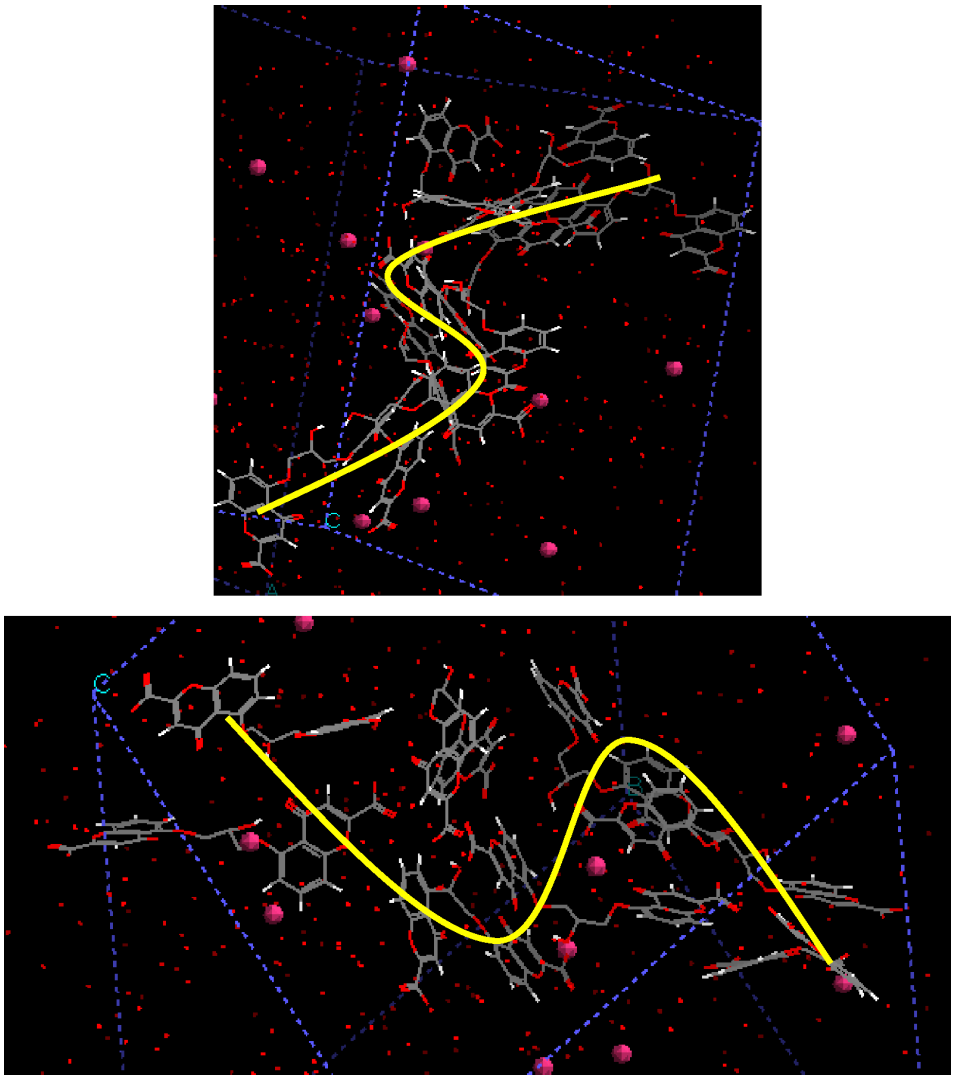

Figure 8. Snapshots of DCNA in water after 200 ps. The molecules form zig-zag structures with intermolecular $\pi-\pi$ interactions.

a circular cross-section as a result of this inter-twining. The diameter of the cross-section is about 2 nm, which is consistent with experimental estimates cited earlier.

6. Energy considerations

The energy profiles of aqueous solutions of carbocyanine dyes are shown in table 1. Delta energy is the change of energy in the assembly of n HFA molecules from their randomly distributed state in a bath of 1000 water molecules, normalized by dividing the energy by n HFA molecules. The units are in kcal/mol of HFA molecules. The bond energy contribution to the total energy is roughly the same with each of the carbocyanine dyes. They somewhat more constrained in water than in vacuum. On the other hand, the bond energy of DCNA is slightly smaller in water. The contribution of the bond energies to the total is, however, quite small in all of these cases.

The Van der Waals and hydrogen bond contributions during self assembly of the carbocyanine systems are quite similar. The difference largely arises from the electrostatic interactions and this can be attributed to the ability of the carbocyanines to π-stack optimally as well as interactions between the self-assembling ions. C8O4 with its longer side chains has greater trouble in optimal orientation of the π-rings and shows the least favorable electrostatic interactions among the carbocyanines. TDBC with the shortest side chains has the most favorable interactions. C8O4 forms a loose helix; TDBC forms a well-connected sheet. In the latter, there are significant interactions between the anions on the side chains resulting in increased electrostatic contributions. C8O3 forms a tight helical network with close $\pi-\pi$ interactions and has stronger electrostatic contributions than C8O4. The carbocyanine dyes also have greater hydrogen-bonding with water, primarily owing to more groups that are capable of forming h-bonds compared to DCNA.

The trajectories of the non-bond energy profile (changing energy with simulation time) are presented in figure 10—the non-bond energy dominates the self-assembly. There is a distinctive feature in all the

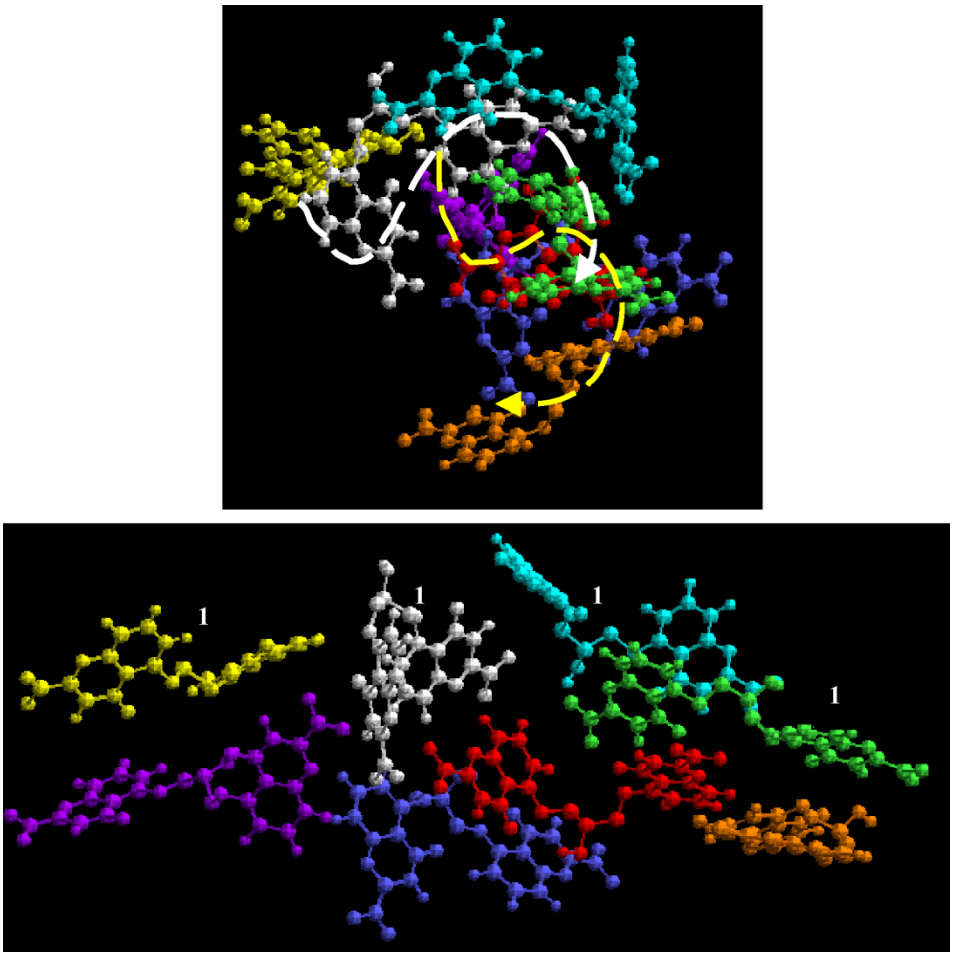

Figure 9. DCNA molecules show two threads that helically inter-twine. One thread is marked with "1" on the bottom figure. The top figure shows the top view of the intertwining helices. Notice the changing orientation of the chromonics molecules.

trajectories—presence of relatively flat regions followed by sharp drops in energy. The flat regions correspond to larger range changes in the cell consisting of reorganization of water molecules around the self-assembly. The sharp drops correspond to significant change in the relative orientations and distances between aromatic rings or interactions between the chromonics molecules and the first water shell. Thus, these sharp drops are largely owing to changes in the water-chromonics or chromonics-chromonics interactions during the course of self-assembly pointing to small changes in position and orientations of the molecules within the stack.

It is significant that the energy of self-assembly is distinctly favorable—self assembly of these molecules is enthalpically driven. Thus, one does not see these molecules behave like surfactants where they are forced to the surface owing to hydrophobic effects.

Table 1. Delta energy of carbocyanine dyes in water. Energy listed in Kcal/mol per HFA.

Energies (Kcal/mol)	*C8O3*	*C8O4*	*TDBC*	*DCNA*
Bond	5.0	5.0	5.0	−6.5
Non-bond	−100.0	−40.0	−110.0	−40.0
H-bond	−30.0	−20.0	−25.0	−15.0
Van der Waals	10.0	10.0	10.0	7.0
Electrostatic	−80.0	−30.0	−95.0	−30.0

The snapshots of self-assembly suggest that the ordered configuration is not a stack of HFA molecules, one above the other, as seen with self-assembled structures of other aromatic complexes. The HFA molecules seem to form daisy chains with aromatic rings of one molecule interacting with aromatic rings of two different molecules. The carbon chain linking the aromatic groups is perhaps the cause of such a self-assembly (as opposed to them stacking on above the other). A carbon chain naturally twists and thus causes the aromatic rings (and thus the entire molecule) to take on a non-planar structure. In such a configuration, it becomes more favorable for the molecules to form a daisy chain rather than a stack. The entropy in a daisy chain is higher than a vertical stack (where the molecules are more constrained). The entropy of such flexible linkers influences the self-assembly of these molecules also affecting the enthalpic dominance in driving self assembly.

There seems to be little difference between the structures of the carbocyanine dyes. On analyzing the snapshots, however, the biggest difference between

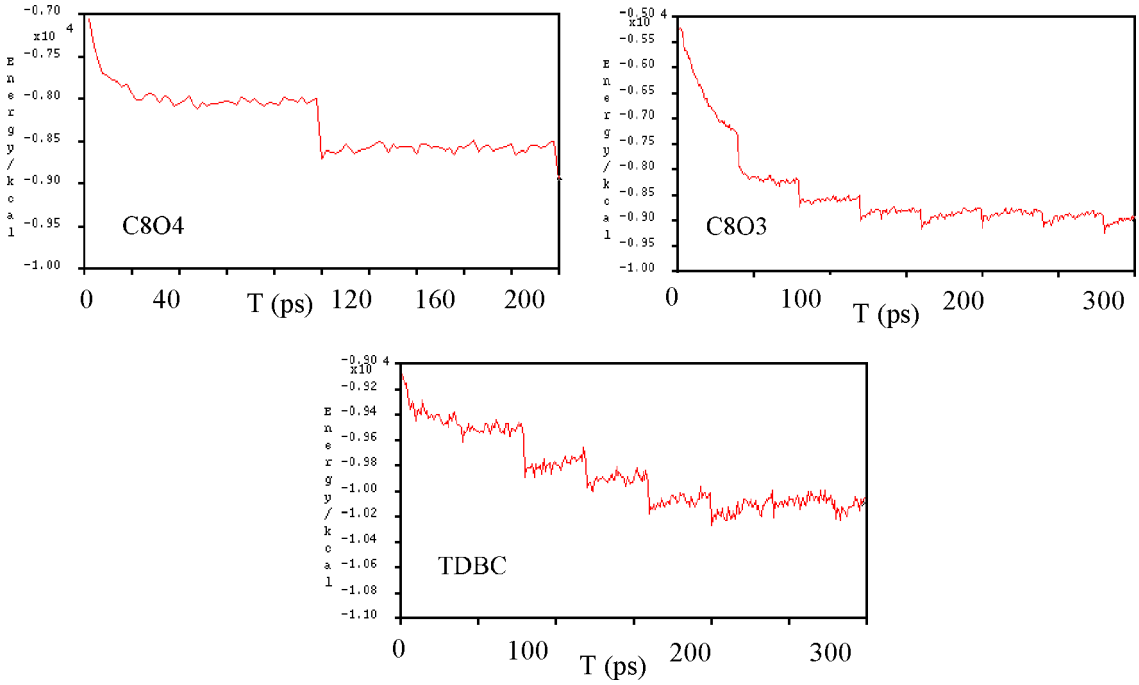

Figure 10. Trajectories of non-bond energy for the carbocyanine dyes. Energy (kcal/unit cell) is presented in simulation units.

the molecular structures of the dyes is the torsion angle between the aromatic rings. While the C8O3 structures show that the aromatic rings are at a torsional angle of about 60°, C8O4 structures show a torsional angle of about 40° and TDBC of about 75°. The primary reason for this difference seems to be the length and character of the side chains. The TDBC with a shorter side chain is more flexible than C8O3 or C8O4. The side chains also affect the molar volume of these systems—TDBC has the smallest molar volume. Interactions between the aromatic rings form the basis of self-assembly. The torsion and the bond angles between the aromatic rings affect the structure of self-assembly.

These hypotheses are borne out in a significantly different system—DCNA. The conjugated aromatic rings are the basis of self-assembly. The torsion angle (at about 90°) is significantly larger and the self-assembled stricture presents a distinct helical nature with multiple threads intertwining. DCNA has a slightly favorable Van der Waals energy compared to the carbocyanine self-assemblies and less favorable coulombic interaction. The spacing between the aromatic rings might be slightly different (smaller by 0.2 Å—though, given the broad peak, this cannot be conclusively claimed) owing to the difference in the nature of the aromatic moieties. Overall, the energies of self-assembly (table 1) are quite similar to the carbocyanine dyes despite significantly different structures—this again points to the dominance of aromatic interactions.

7. Summary

These examples suggest guidelines for assembly of HFA molecules. The pitch of the helical structure formed by a ribbon could be controlled by the nature of the linker between the two aromatic groups. Clearly, the length of the side chains and their functionality affect the structure of the self-assembly as well as the energy of interactions. Use of hydrogen bonding groups, as opposed to anionic groups, affects the ability to form sheets (as opposed to cross linking networks) as well as the strength or size of those self-assembling sheets.

Based on these systems, it can be concluded that the structure connecting the aromatic rings is critical in the self-assembled order of these lyotropic molecules. Changing linker structure or side chains affects the orientation of these aromatic rings with respect to each other, as well as the interactions between self-assembled clusters.

Acknowledgements

The author would like to thank Drs Hassan Sahouani, Allen Siedle, Manish Jain, Gregg Caldwell and Shih-Hung Chou for insightful discussions regarding the nature of these molecules and the mechanisms involved in self assembly.

References

[1] C. Tanford. *The Hydrophobic Effect: Formation of Micelles and Biological Membranes*, John Wiley & Sons, New York (1973).
[2] J. Lydon. *Handbook of Liquid Crystals*, Volume 2B, pp. 981–1007 (1998).
[3] E.A. Meyer, R.K. Castellano, F. Diedrich. Interactions with aromatic rings in chemical and biological recognition. *Angew. Chem. Int. Ed.*, **42**(11), 1211 (2003).

[4] H. Berlepsch, C. von Bottcher, A. Ouart, C. Burger, S. Dahne, S. Kirstein. Supramolecular structures of J-aggregates of carbocyanine dyes in solution. *J. Phys. Chem. B*, **104**(22), 5255 (2000).
[5] F. Wurthner, S. Yao, U. Beginn. Highly ordered merocyanine dye assemblies by supramolecular polymerization and hierarchical self-organization. *Angew. Chem. Int. Ed.*, **42**, 3247 (2003).
[6] N.H. Hartshorne, G.D. Woodard. Mesomorphism in the system disodium chromoglcyate - water. *Mol. Cryst. Liq. Cryst.*, **23**, 343 (1973).
[7] S. Makio, N. Kanamaru, J. Tanaka. The J-aggregate 5, 5′, 6, 6′-tetrachloro -1, 1′-diethyl-3,3′-bis (4 -sulfobutyl) benzimidazolocarbocyanine sodium salt in aqueous solution. *Bull. Chem. Soc. Jpn.*, **53**, 3120 (1980).
[8] A. Pawlik, S. Kirstein, U. De Rossi, S. Dahne. Structural conditions for spontaneous generation of optical activity in J-aggregates. *J. Phys. Chem. B*, **101**, 5646 (1997).
[9] U. De Rossi, J. Moll, M. Spieles, G. Bach, S. Dahne, J. Kriwanek, M. Lisk. Control of the J-aggregation phenomenon by variation of the N-alkyl-substituents. *J. Prakt. Chem.*, **337**, 203 (1995).
[10] U. De Rossi, S. Dahne, S.C.J. Meskers, H.P.J.M. Dekkers. spontane bildung vol optischer aktivität in J-aggregaten mit davydov-aufsplatung. *Angew. Chem.*, **108**, 827 (1996).
[11] H. Lee, M.M. Labes. Lyotropic cholesteric and nematic phases of disodium chromoglycate in magnetic fields. *Mol. Cryst. Liq. Cryst.*, **84**, 137 (1982).
[12] J. Lydon. New models for mesophases of disodium chromoglycate. *Mol. Cryst. Liq. Cryst.*, **64**, 19 (1980).
[13] M. Kobayashi, A. Sasagawa, T. Hoshi, J. Okubo. High-order aggregation of crystal violet in the chromonic lyotropic mesophases of 7,7′-disodiumchromoglycate. *Mol. Cryst. Liq. Cryst.*, **225**, 293 (1993).